

See discussions, stats, and author profiles for this publication at: <https://www.researchgate.net/publication/230671962>

# A Novel Approach to the Discovery of Small-Molecule Ligands of CDK2

ARTICLE *in* CHEMBIOCHEM · SEPTEMBER 2012

Impact Factor: 3.09 · DOI: 10.1002/cbic.201200316 · Source: PubMed

---

CITATIONS

20

---

READS

30

6 AUTHORS, INCLUDING:



**Stephane Betzi**

French National Centre for Scientific Research

**24** PUBLICATIONS **417** CITATIONS

SEE PROFILE



**Donna J. Ingles**

Moffitt Cancer Center

**15** PUBLICATIONS **159** CITATIONS

SEE PROFILE



**Jinyi Zhu**

Moffitt Cancer Center

**16** PUBLICATIONS **164** CITATIONS

SEE PROFILE

Published in final edited form as:

*Chembiochem*. 2012 September 24; 13(14): 2128–2136. doi:10.1002/cbic.201200316.

## A novel approach to the discovery of small molecule ligands of CDK2

**Dr. Mathew P. Martin<sup>#</sup>, Mr. Riazul Alam<sup>#</sup>, Dr. Stephane Betzi, Mrs. Donna J. Ingles, Dr. Jin-Yi Zhu, and Prof. Ernst Schönbrunn**

Drug Discovery Department, Moffitt Cancer Center and Research Institute, 12902 Magnolia Drive, Tampa, FL 33612 (USA), Fax: (+1)813 745 6748

Ernst Schönbrunn: ernst.schonbrunn@moffitt.org

### Abstract

In an attempt to identify novel small molecule ligands of CDK2 with potential as allosteric inhibitors, we devised a robust *and cost-effective* fluorescence-based high-throughput screening assay. The assay is based on the specific interaction of CDK2 with the extrinsic fluorophore 8-anilino-1-naphthalene sulfonate (ANS), which binds to a large allosteric pocket adjacent to the ATP site. Hit compounds which displace ANS directly or indirectly from CDK2 are readily classified as ATP site binders or allosteric ligands through the use of staurosporine, which blocks the ATP site without displacing ANS. Pilot screening of 1,453 compounds led to the discovery of 12 compounds with displacement activities ( $EC_{50}$  values) ranging from 6 to 44  $\mu$ M, all of which were classified as ATP site-directed ligands. Four new Type I inhibitor scaffolds were confirmed by X-ray crystallography. While this small compound library contained only ATP-site directed ligands, the application of this assay to large compound libraries has the potential to reveal previously unrecognized chemical scaffolds suitable for structure-based design of CDK2 inhibitors with new mechanisms of action.

### Keywords

high-throughput screening; drug discovery; chemical probes; allosteric inhibitors; protein-protein interaction inhibitors

### Introduction

Cyclin-dependent kinases (CDKs) are members of the serine/threonine kinase family and are key enzymes in cell cycle progression and transcription. Deregulation of CDKs has been implicated in a number of diseases, ranging from inflammation to neurodegenerative diseases to cancer. <sup>[1]</sup> The CDK2-cyclin A complex predominantly controls the G1- to S-phase checkpoint <sup>[2]</sup> and, therefore, represents an attractive target for therapeutics designed to arrest or recover control of the cell cycle in aberrantly dividing cells <sup>[3]</sup>. Prominent CDK2 inhibitors such as flavopiridol have not been successful in clinical trials due to low specificity towards other CDKs, resulting in undesirable off-target interactions. <sup>[4]</sup> Known CDK2 inhibitors exclusively belong to the Type I class of kinase inhibitors, which directly compete with ATP for binding to the active site. These inhibitors often do not effectively discriminate between multiple kinases indicating that the greatest promise for clinical potential resides with inhibitors that exert novel mechanisms of action. Protein kinases such

Correspondence to: Ernst Schönbrunn, ernst.schonbrunn@moffitt.org.

<sup>#</sup>Authors contributed equally

as Abl [5], p38 [6], and MEK1 [7] have been successfully targeted by inhibitors with allosteric properties which bind to a hydrophobic pocket adjacent to the ATP site. Type II inhibitors, such as imatinib (Gleevec) for Abl, extend from the ATP site into this hydrophobic pocket, whereas Type III inhibitors of MEK1 are purely allosteric. Binding of Type II or Type III inhibitors is often accompanied by significant structural changes of the highly conserved DFG (Asp-Phe-Gly) motif.

CDKs are unique among protein kinases, as their functionality strictly depends on the association with their partner proteins, the cyclins. The CDK2-cyclin A complex is relatively tight ( $K_d = 0.6 \mu\text{M}$ ) [8], and small molecule inhibitors able to effectively disrupt this protein-protein interaction (PPI) have not been identified to date. CDK2 undergoes large conformational changes upon binding of cyclins, particularly of the PSTAIRE helix (C-helix), which is central to efficient complex formation [9]. Migration of the C-helix upon complex formation narrows a large hydrophobic pocket that exists in free CDK2, approximately midway between the ATP site and the C-helix. We recently reported that the extrinsic fluorophore 8-anilinoanthracene-1-sulfonate (ANS) specifically interacts with CDK2 by binding to this hydrophobic pocket and stabilizing an enzyme conformation that is incompatible for interaction with cyclins. [8] The data suggested that compounds able to displace ANS from CDK2 have potential as allosteric inhibitors able to disrupt the CDK2-cyclin A interaction.

Previously reported high-throughput screening (HTS) campaigns for inhibitors have all essentially followed similar approaches, using activity assays to identify inhibitors of the CDK2-cyclin A catalytic reaction. [10] In an attempt to identify new small molecule ligands with potential as allosteric inhibitors, we devised a robust and cost-effective fluorescence-based HTS assay that detects compounds able to displace ANS from the allosteric site. Screening of a small library of 1,453 compounds from the National Cancer Institute (NCI) led to the discovery of 12 previously unknown ligands of CDK2, all of which were classified as Type I ligands by binding to the ATP site, indicating that the library screened is void of compounds with allosteric binding potential towards CDK2. The data suggest suitability of this assay for the screening of larger compound libraries with the specific intention of identifying allosteric small molecule ligands.

## Results and Discussion

### Development of an ANS displacement assay in HTS format

We previously reported that ANS specifically interacts with CDK2 by binding to a large allosteric pocket adjacent to the ATP site [8]. We also described the way in which certain Type I inhibitors such as SU9516 ( $\text{IC}_{50} = 0.13 \mu\text{M}$ ) displace ANS by inducing conformational changes around the DFG motif, which is bordered at either end by the ATP and ANS sites. Other Type I inhibitors such as JWS648 ( $\text{IC}_{50} = 5.9 \mu\text{M}$ ) rendered the ANS site unchanged and, therefore, did not displace ANS. The CDK2-ANS interaction thus presents a unique opportunity for the design of a cost-effective HTS campaign to discover Type I, II, and III ligands (Fig. 1). We therefore configured an HTS-compatible assay suitable for the screening of compounds with ANS displacement potential, as measured by dose-dependent quenching of the CDK2-ANS fluorescence yield. The use of CDK2 alone allows for the identification of compounds that bind to the ATP site (Type I and Type II ligands) and displace ANS indirectly, as well as those that compete directly with ANS for binding to the allosteric site (Type III inhibitors). To distinguish allosteric from ATP site-directed ligands, a follow-up assay is employed in which a potent Type I inhibitor with weak ANS displacement potential serves to block the ATP site. Hit compounds are further analyzed for inhibitory potential against the CDK2-cyclin A complex, and selected compounds are co-crystallized with CDK2 for structure determination (Fig. 1C). This

approach enables identification, classification, and verification of new chemical scaffolds as potential lead compounds for the future development of efficacious CDK2 inhibitors with novel mechanisms of action.

The CDK2-ANS assay is based upon the fluorescent signal emitted from the interaction of ANS within the allosteric pocket of CDK2. Our previous benchtop experiments were conducted in a 1×1 mL cuvette, and the fluorescent signal of the CDK2-ANS solution was recorded at excitation and emission wavelengths of 360 nm and 460 nm, respectively.<sup>[8]</sup> To achieve HTS compatibility, the assay volume was scaled down from 1 ml to a 50  $\mu$ L 96-well plate format, with the resulting titration of ANS into CDK2 yielding a  $K_{d(app)}$  of 21  $\pm$  1.3  $\mu$ M (Supplemental Fig. 1A). ANS and CDK2 concentrations of 50  $\mu$ M and 1.6  $\mu$ M (0.05 mg/mL), respectively, in buffer containing 40 mM HEPES (pH 7.5) were deemed optimal for the final assay. A control experiment using compound SU9516 (displacer, positive control) was conducted under these assay conditions yielding an  $EC_{50}$  value of 0.8  $\mu$ M. The  $K_{d(app)}$  (ANS) and  $EC_{50}$  (SU9516) values were consistent with our previously reported data using a 1×1 mL volume cuvette format.<sup>[8]</sup> In order to establish the robustness and reliability of our assay for use in HTS, parameters such as enzyme stability and the permitted percentage of DMSO were examined. Stock solutions of CDK2 at 16  $\mu$ M (0.5 mg/ml) remained stable for up to four hours on ice prior to 1:10 dilution into the assay mixture. Titration of DMSO from 1 % to 20 % showed a reduction in the fluorescence yield of CDK2-ANS; however, DMSO had no effect on the displacement activity of SU9516 (Supplemental Fig. 1B). Therefore, a DMSO concentration of 5 % was considered acceptable for the assay. For large HTS campaigns, the use of a detergent in the assay mixture is advantageous to avoid false positive hits caused by colloidal aggregates<sup>[11]</sup>. We therefore performed additional experiments to test the robustness of the assay in the presence of 0.005 and 0.01% Triton X100, concentrations typically used in HTS campaigns. Inclusion of detergent in the assay mixture did not affect the fluorescent yield of the CDK2-ANS complex or the quenching potential of inhibitors such as SU9516 (Supplemental Fig. 1C). As the small NIH libraries screened as part of this work consisted of well-characterized and freshly prepared compounds, we abstained from addition of detergent in the assay.

### Screening of National Cancer Institute libraries

A pilot screen using the NCI Oncology set of 89 compounds was conducted in order to assess the quality of the CDK2-ANS assay in a half-area 96-well format. The Z-factor for the pilot screen was 0.85, with positive (SU9516) and negative (5 % DMSO) controls. During screening, it was noted that two innate properties of small molecules in the library, intrinsic fluorescence and absorbance at the excitation or emission wavelengths, needed to be considered to ensure accuracy of the results and correct interpretation of the data. Use of an excitation filter of 405 nm provided a significant advantage over the previously used wavelength of 360 nm. Although the CDK2-ANS complex yields a maximal fluorescence emission signal at 460 nm after excitation at 360 nm, many compounds from the library screened displayed intrinsic fluorescence when excited in the 340–380 nm range, while only a fraction of these displayed fluorescence when excited at 405 nm. In order to correct for the inner-filter effect, which causes a reduction in fluorescence signal for compounds with high absorbance, optical density readings were taken at the excitation and emission wavelengths for each well prior to addition of CDK2. Data correction (see Experimental Section) enabled identification, and thus exclusion, of false positive hit compounds that unspecifically quenched the CDK2-ANS fluorescence (Fig. 2).

Following optimization of the CDK2-ANS assay and confirmation of reliability from the NCI Oncology set pilot screen, compounds from the NCI Diversity II library were screened using the half-area 96-well CDK2-ANS assay format. Each compound was tested at a concentration of 100  $\mu$ M with a final DMSO concentration of 5 %; those showing at least 60

% displacement were considered hits. Overall, the 1,453 compounds from these two NCI libraries yielded a hit rate of 1.4 % with an average Z-factor of 0.78 and a signal-to-background ratio of 12 (Fig. 3A). These characteristics suggest excellent assay performance<sup>[12]</sup> and indicate feasibility for further development into 384- or 1536-well format. Hit compounds were confirmed in dose-response titrations, resulting in 12 compounds with EC<sub>50</sub> values below 50  $\mu$ M (Table 1) (Supplemental Fig. 2). Inhibitory potential of the hit compounds against activated CDK2-cyclin A was weak, and only purpurogallin (**2**) (IC<sub>50</sub> = 17  $\mu$ M) and compounds **4**, **5**, and **6** (IC<sub>50</sub> ~ 50  $\mu$ M) displayed appreciable inhibitory activity (Table 1). Two hits from the NCI Oncology set were identified as known Type I tyrosine kinase inhibitors sunitinib (**1**)<sup>[13]</sup> and sorafenib (**8**)<sup>[14]</sup>, the former of which was previously reported as a weak inhibitor of CDK1 (IC<sub>50</sub> = 2.6  $\mu$ M)<sup>[15]</sup>.

### Classification of Type I/II and Type III ligands

In order to differentiate between ATP-competitive ligands (Type I and Type II) and those with allosteric binding potential (Type III), we probed known high-affinity CDK2 inhibitors for their suitability to block the ATP site without displacing ANS. The presence of such an ATP site plug should result in a significant shift of the dose-response curves to higher EC<sub>50</sub> values for ligands with Type I and Type II binding potential, whereas EC<sub>50</sub> values for Type III ligands remain unaltered. The previously studied inhibitor JWS648 has an IC<sub>50</sub> value of 5.9  $\mu$ M<sup>[8]</sup> and binds to the CDK2-ANS complex without perturbing the allosteric site, even at high concentrations (up to 100  $\mu$ M). However, JWS648 is not a very effective ATP site blocker, as EC<sub>50</sub> values for SU9516 increase only by a factor of 4 in the presence of 50  $\mu$ M JWS648<sup>[8]</sup>. Selective screening for purely allosteric ligands necessitates blocking the active site more effectively with a high affinity Type I inhibitor. The commercially available pan-kinase inhibitor staurosporine (IC<sub>50</sub> = 7 nM)<sup>[16]</sup> was a suitable candidate to replace JWS648, as it too enables the fluorescent CDK2-ANS complex to remain intact even at high concentrations (Fig. 3B). Titration of SU9516 in the presence of 10  $\mu$ M staurosporine resulted in a 15-fold increase in EC<sub>50</sub> value from 0.8 to 12  $\mu$ M.

To verify that staurosporine is a suitable ATP site plug for hit classification, we determined the crystal structure of CDK2 with staurosporine alone and in ternary complex with ANS (Fig. 4) (Supplemental Fig. 3 and 4). Staurosporine binds to free CDK2 in the same manner as previously described.<sup>[17]</sup> In the ternary complex, two ANS molecules are bound to the allosteric pocket adjacent to staurosporine, similar to the ternary complex of JWS648 with ANS.<sup>[8]</sup> All hit compounds displayed significantly increased EC<sub>50</sub> values in the presence of 10  $\mu$ M staurosporine, indicating that compound activity is restricted to the ATP site (Table 1). It appears that the NCI libraries screened here did not contain small molecule ligands with allosteric binding potential towards CDK2.

### Validation of hit compounds

To determine the binding mode of hit compounds at the molecular level, we next pursued co-crystal structure determination with CDK2. Sunitinib (**1**) (Fig. 5A) is a Type I inhibitor of a number of kinases, including human phosphorylase kinase  $\gamma$ 2 (2Y7J, no associated publication), ITK (3MIY<sup>[18]</sup>), and KIT (3G0E<sup>[19]</sup>). However, the crystal structure of sunitinib liganded with CDK2 was not previously available. As expected, sunitinib binds to CDK2 through hydrogen bonding interactions with the hinge region of the ATP site, namely the backbone of residues Glu81 and Leu83. The complex is further stabilized through van der Waals (hydrophobic) interactions with gatekeeper residues Phe80 and Ile10. The triethylamine moiety projects toward solvent, and the fluorindole moiety points towards the DFG motif. Hit compounds **2**, **3**, and **4** have not been previously identified as ligands of CDK2. Compound **2**, known as purpurogallin, was previously modeled as an inhibitor of

Polo-like kinase [20]; however, this is the first reported enzyme-bound crystal structure of purpurogallin (Fig. 5B). The three hydroxyl groups of the six-membered ring bind to the hinge region (Glu81 and Leu83) through hydrogen bonding interactions (Fig. 5B). Hit compound **3** forms a single hydrogen bond with the main chain of Leu83 and a series of hydrophobic interactions with Leu134 and Phe80 (Fig. 5C). Hit compound **4** forms two potential hydrogen bonds through the hinge (Glu81 and Leu83) (Fig. 5D). Compound **4** is also stabilized through hydrophobic interactions with Ile10 and Leu134. Common to hit compounds **1–4** is an imperfect fit to the ATP site, which explains their disruptive effect on the CDK2-ANS complex. Potential steric clashes exist between each compound and Phe80 or Asp145 (Fig. 5), residues that constitute both the ATP site and the allosteric pocket (Fig. 4). While inhibitors such as staurosporine are able to bind to the ATP site alongside ANS, Type I ligands such as the compounds identified here, induce conformational changes to the DFG motif and/or Phe80, thereby impacting the structural integrity of the ANS binding pocket.

## Conclusion

We describe the development of a novel, robust, and cost-effective HTS assay for the identification of small molecule ligands of CDK2. This assay targets free, unphosphorylated CDK2 as opposed to the activated CDK2-cyclin A complex typically used in screening campaigns. Data evaluation involves inner-filter correction to readily identify false positive hits, and a follow-up assay has been devised to further classify hit compounds as ATP site-directed (Type I and Type II) or allosteric ligands (Type III). The small library of 1,453 compounds screened did not reveal ligands with allosteric binding potential to CDK2. However, new Type I ligands were discovered, four of which were verified by crystallography. Application of this assay to large compound libraries has the potential to reveal previously unrecognized chemical scaffolds suitable for the structure-based design of CDK2 inhibitors with novel mechanisms of action.

Free CDK2 displays significant conformational flexibility and accommodates the binding of highly diverse small molecule ligands. Compounds that bind to the ANS site and stabilize a CDK2 conformation incapable of efficiently interacting with cyclins have potential as allosteric protein-protein interaction inhibitors. ANS has a relatively weak binding affinity to CDK2 ( $K_d = 21 \mu\text{M}$ ), which renders its binding site, particularly the DFG motif, vulnerable to conformational changes induced by ATP site-directed ligands. Selective screening for purely allosteric ligands can be achieved by blocking the ATP site with a Type I inhibitor with weak ANS displacement potential but high affinity, such as staurosporine. An alternative approach is the design of ANS analogues as high-affinity fluorescence probes of CDK2, in order to stabilize the fluorescent complex against unwanted conformational changes caused by Type I ligands.

## Experimental Section

### Reagents and compounds

Reagents and compounds were purchased from Sigma–Aldrich (St. Louis, MO) and Hampton Research (Aliso Viejo, CA) unless otherwise indicated. The peptide substrate PKTPKKAKKL [10a] for activity assays was obtained from Biomatik (Wilmington, DE). CDK2 inhibitor SU9516 and staurosporine was purchased from Tocris Bioscience (Ellisville, MO).



## Protein purification and crystallography

Human full length CDK2 was overexpressed in *E. coli* cells with a GST tag and purified through a combination affinity and size exclusion chromatography as previously reported [8]. CDK2 was co-crystallized with hit compounds **1**, **2**, and **3** as described previously [8]. The crystal structure with compound **4** was obtained by in-diffusion of free CDK2 crystals with 2 mM compound for 24 h in harvesting buffer, prior to data collection [8]. The crystal structure with staurosporine was obtained in the same manner. The ternary CDK2-staurosporine-ANS complex was obtained through in-diffusion of CDK2-staurosporine crystals with 10mM ANS overnight. X-ray diffraction data were recorded at  $-180^{\circ}\text{C}$  using  $\text{CuK}\alpha$  radiation generated by a Rigaku Micro-Max 007-HF rotating anode (MSC, The Woodlands, TX) using a CCD Saturn 944+ in the Moffitt Structural Biology Core facility. Data were reduced with XDS [21]. The structure was solved by molecular replacement using the MolRep program from CCP4 [22] with the pdb 3PXZ as a starting model. PHENIX [23] was employed for refinement, and model building was performed using Coot [24]. Data and refinement statistics for all deposited structures are shown in Table 2. Figures were prepared using PyMOL [25].

## CDK2-ANS displacement assay in 96-well format

The CDK2-ANS assay was configured for 96-well plate format with a final volume of 50  $\mu\text{L}$ . Components were added to each well using a Biomek FX liquid handling system equipped with a 96-well dispensing head (Beckman Coulter, Brea, CA). Initially, 40  $\mu\text{L}$  of a solution containing 62.5  $\mu\text{M}$  ANS (at saturation) in 50 mM HEPES (pH 7.5) with 1 mM DTT was aliquoted into each well of a black 96-well area assay plate (Corning, Corning, NY). Screening compound (5  $\mu\text{L}$  of 1 mM in 50% DMSO) was added to each well, resulting in a final compound concentration of 100  $\mu\text{M}$  (in 5% DMSO). Plates were read using a Wallac Envision 2102 plate reader (Perkin Elmer, Waltham, MA) with excitation and emission filters corresponding to 405 nm and 460 nm, respectively, to obtain background fluorescence measurements ( $F_{\text{BLANK}}$ ) for detecting compounds with inherent fluorescence (Fig. 2A). CDK2 (5  $\mu\text{L}$  of a 16  $\mu\text{M}$  stock solution) was then added to each well to yield a final concentration of 1.6  $\mu\text{M}$ . The plate was read a second time ( $F_{\text{RAW}}$ ) (Fig. 2B), and the observed fluorescence signal ( $\Delta F_{(460\text{nm})}$ ) (Fig. 2C) was determined using Equation 1.

$$\Delta F_{(460\text{nm})} = F_{\text{RAW}} - F_{\text{BLANK}} \quad \text{Equation (1)}$$

$$F_{\text{CORR}} = \Delta F \times 10^{\left(\frac{\text{OD}_{\text{ex}} + \text{OD}_{\text{em}}}{2}\right)} \quad \text{Equation (2)}$$

$$\%F_{\text{CORR}} = \frac{1}{1 + \left(\frac{[I]}{EC_{50}}\right)^n} \quad \text{Equation (3)}$$

$$Z_{\text{FACTOR}} = 1 - \frac{3(\sigma_s + \sigma_c)}{|\mu_s - \mu_c|} \quad \text{Equation (4)}$$

The contents of each well were then transferred to clear 96-well plates (Corning), and absorbance was measured at both excitation (405nm) and emission (460nm) wavelengths using a SpectraMax 340PC plate reader (Molecular Devices, Sunnyvale, CA). Data were corrected for the inner filter effect using Equation 2, where  $\text{OD}_{\text{ex}}$  and  $\text{OD}_{\text{em}}$  are the optical density values at extinction and emission wavelengths, respectively [26]. Use of Equation 2 gives a reasonable approximation of true ANS quenching potential of compounds regardless

of plate brand or format (96, 384, or 1536) (Fig. 2D). SU9516 (10  $\mu$ M final concentration) and 5 % (v/v) DMSO were used as controls representing 100 % and 0 % displacement potential, respectively. Potential hits were further confirmed through an eight-point EC<sub>50</sub> titration over a concentration range of 0.01–100  $\mu$ M using the same assay design and fitting the data to Equation 3, where [L] is the concentration of the inhibitor and  $n$  is the Hill slope coefficient. Z-factor values for assay performance were calculated using Equation 4, where  $\sigma_s$  is the standard deviation of samples,  $\sigma_c$  is the standard deviation of controls,  $\mu_s$  is the mean values of samples, and  $\mu_c$  is the mean value of controls [12]. For classification, hit compounds were subjected to an eight-point competition titration (0.01–100  $\mu$ M) in the presence of staurosporine (5 and 10  $\mu$ M). The assay was conducted at room temperature under controlled lighting, allowing the ANS signal to be stable for up to 1 hour; however, all measurements were taken directly after addition of components. Inhibitory potential of the hit compounds against the activated CDK2-cyclin A2 complex was determined using the ADP Quest fluorescence assay (DiscoverX, Fremont, CA) as previously described [8, 27].

## Additional Information

The atomic coordinates and structure factors for the crystal structures determined as part of this work have been deposited in the Protein Data Bank (entries 3TI1, 3TIY, 3TIZ, 4EZ3, 4EZ7, and 4ERW).

## Supplementary Material

Refer to Web version on PubMed Central for supplementary material.

## Acknowledgments

This work was supported in part by National Institutes of Health Grant U54-HD055763. We thank the Moffitt Chemical Biology Core for use of their X-ray crystallography and HTS facilities.

## References

1. a) Johnson LN. Quarterly reviews of biophysics. 2009; 42:1–40. [PubMed: 19296866] b) Hall M, Peters G. Adv Cancer Res. 1996; 68:67–108. [PubMed: 8712071] c) Zhang J, Yang PL, Gray NS. Nat Rev Cancer. 2009; 9:28–39. [PubMed: 19104514] d) Bain J, Plater L, Elliott M, Shpiro N, Hastie CJ, McLauchlan H, Klevernic I, Arthur JS, Alessi DR, Cohen P. Biochem J. 2007; 408:297–315. [PubMed: 17850214]
2. a) Ortega S, Malumbres M, Barbacid M. Biochim Biophys Acta. 2002; 1602:73–87. [PubMed: 11960696] b) Weinberg RA. Cell. 1995; 81:323–330. [PubMed: 7736585]
3. Horiuchi D, Huskey NE, Kusdra L, Wohlbold L, Merrick KA, Zhang C, Creasman KJ, Shokat KM, Fisher RP, Goga A. Proc Natl Acad Sci U S A. 2012; 109:E1019–1027. [PubMed: 22474407]
4. a) Echalié A, Endicott JA, Noble ME. Biochim Biophys Acta. 2010; 1804:511–519. [PubMed: 19822225] b) Shapiro GI. Clinical Cancer Research. 2004; 10:4270s–4275s. [PubMed: 15217973]
5. Cowan-Jacob SW, Fendrich G, Floersheimer A, Furet P, Liebetanz J, Rummel G, Rheinberger P, Centeleghe M, Fabbro D, Manley PW. Acta Crystallogr D Biol Crystallogr. 2007; 63:80–93. [PubMed: 17164530]
6. Angell RM, Angell TD, Bamborough P, Bamford MJ, Chung CW, Cockerill SG, Flack SS, Jones KL, Laine DI, Longstaff T, Ludbrook S, Pearson R, Smith KJ, Smee PA, Somers DO, Walker AL. Bioorganic & medicinal chemistry letters. 2008; 18:4433–4437. [PubMed: 18602262]
7. Ohren JF, Chen H, Pavlovsky A, Whitehead C, Zhang E, Kuffa P, Yan C, McConnell P, Spessard C, Banotai C, Mueller WT, Delaney A, Omer C, Sebolt-Leopold J, Dudley DT, Leung IK, Flamme C, Warmus J, Kaufman M, Barrett S, Tecle H, Hasemann CA. Nat Struct Mol Biol. 2004; 11:1192–1197. [PubMed: 15543157]



8. Betzi S, Alam R, Martin MP, Lubbers DJ, Han H, Jakkaraj SR, Georg GI, Schonbrunn E. *ACS Chem Biol*. 2011; 6:492–501. [PubMed: 21291269]
9. a) Brown NR, Noble ME, Endicott JA, Garman EF, Wakatsuki S, Mitchell E, Rasmussen B, Hunt T, Johnson LN. *Structure*. 1995; 3:1235–1247. [PubMed: 8591034] b) Echalié A, Endicott JA, Noble ME. *Biochimica et biophysica acta*. 2010; 1804:511–519. [PubMed: 19822225] c) Ruchel R, Schaffrinski M, Schobert P. *Mycoses*. 1995; 38(Suppl 1):28–32. [PubMed: 7630367]
10. a) Stevenson-Lindert LM, Fowler P, Lew J. *J Biol Chem*. 2003; 278:50956–50960. [PubMed: 14506259] b) Stevenson LM, Deal MS, Hagopian JC, Lew J. *Biochemistry*. 2002; 41:8528–8534. [PubMed: 12081504] c) Mettey Y, Gompel M, Thomas V, Garnier M, Leost M, Ceballos-Picot I, Noble M, Endicott J, Vierfond JM, Meijer L. *J Med Chem*. 2003; 46:222–236. [PubMed: 12519061]
11. Jadhav A, Ferreira RS, Klumpp C, Mott BT, Austin CP, Inglese J, Thomas CJ, Maloney DJ, Shoichet BK, Simeonov A. *Journal of medicinal chemistry*. 2010; 53:37–51. [PubMed: 19908840]
12. Zhang JH, Chung TD, Oldenburg KR. *J Biomol Screen*. 1999; 4:67–73. [PubMed: 10838414]
13. Papaetis GS, Syrigos KN. *BioDrugs*. 2009; 23:377–389. [PubMed: 19894779]
14. Wilhelm S, Carter C, Lynch M, Lowinger T, Dumas J, Smith RA, Schwartz B, Simantov R, Kelley S. *Nature reviews Drug discovery*. 2006; 5:835–844.
15. Mendel DB, Laird AD, Xin X, Louie SG, Christensen JG, Li G, Schreck RE, Abrams TJ, Ngai TJ, Lee LB, Murray LJ, Carver J, Chan E, Moss KG, Haznedar JO, Sukbuntherng J, Blake RA, Sun L, Tang C, Miller T, Shirazian S, McMahon G, Cherrington JM. *Clinical cancer research : an official journal of the American Association for Cancer Research*. 2003; 9:327–337. [PubMed: 12538485]
16. a) Gadbois DM, Hamaguchi JR, Swank RA, Bradbury EM. *Biochemical and biophysical research communications*. 1992; 184:80–85. [PubMed: 1567459] b) Meijer L. *Trends in cell biology*. 1996; 6:393–397. [PubMed: 15157522]
17. Lawrie AM, Noble ME, Tunnah P, Brown NR, Johnson LN, Endicott JA. *Nature structural biology*. 1997; 4:796–801.
18. Kutach AK, Villasenor AG, Lam D, Belunis C, Janson C, Lok S, Hong LN, Liu CM, Deval J, Novak TJ, Barnett JW, Chu W, Shaw D, Kuglstatler A. *Chem Biol Drug Des*. 2010; 76:154–163. [PubMed: 20545945]
19. Gajiwala KS, Wu JC, Christensen J, Deshmukh GD, Diehl W, DiNitto JP, English JM, Greig MJ, He YA, Jacques SL, Lunney EA, McTigue M, Molina D, Quenzer T, Wells PA, Yu X, Zhang Y, Zou A, Emmett MR, Marshall AG, Zhang HM, Demetri GD. *Proceedings of the National Academy of Sciences of the United States of America*. 2009; 106:1542–1547. [PubMed: 19164557]
20. Liao C, Park JE, Bang JK, Nicklaus MC, Lee KS. *ACS medicinal chemistry letters*. 2010; 1:110–114. [PubMed: 20625469]
21. Kabsch W. *Journal of Applied Crystallography*. 1993; 26:795–800.
22. *Acta crystallographica. Section D, Biological crystallography*. 1994; 50:760–763.
23. Adams PD, Afonine PV, Bunkoczi G, Chen VB, Davis IW, Echols N, Headd JJ, Hung LW, Kapral GJ, Grosse-Kunstleve RW, McCoy AJ, Moriarty NW, Oeffner R, Read RJ, Richardson DC, Richardson JS, Terwilliger TC, Zwart PH. *Acta crystallographica Section D, Biological crystallography*. 2010; 66:213–221.
24. Emsley P, Cowtan K. *Acta Crystallogr D Biol Crystallogr*. 2004; 60:2126–2132. [PubMed: 15572765]
25. DeLano, WL. DeLano Scientific LLC; Palo Alto, CA, USA: 2008. <http://www.pymol.org>
26. a) Lakowicz, JR. *Principles of Fluorescence Spectroscopy*. Kluwer-Plenum Press; New York: 1999. b) Puchalski MM, Morra MJ, Wandruszka R. *Fresenius' Journal of Analytical Chemistry*. 1991; 340:341–344. c) Rawat SS, Kelkar DA, Chattopadhyay A. *Biophysical journal*. 2004; 87:831–843. [PubMed: 15298892]
27. Martin MP, Zhu JY, Lawrence HR, Pireddu R, Luo Y, Alam R, Ozcan S, Sebt SM, Lawrence NJ, Schonbrunn E. *ACS chemical biology*. 2012

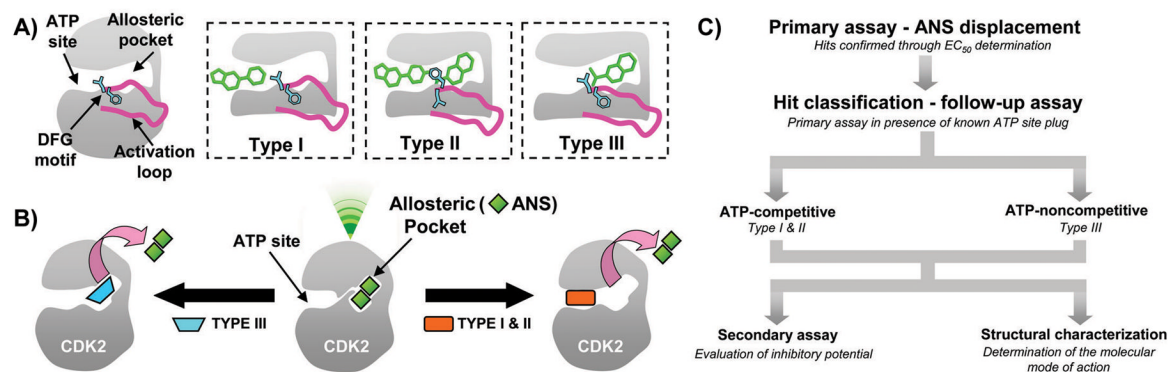


**Figure 1. Exploitation of the CDK2-ANS interaction for the identification of small molecule ligands**

A) Type I kinase inhibitors bind to the ATP site, Type II inhibitors extend from the ATP site into the neighboring allosteric pocket, and Type III inhibitors bind in a purely allosteric manner. The activation loop is shown in magenta, the DFG motif in cyan, and inhibitors in green. B) The allosteric site in CDK2 accommodates two ANS molecules, which are displaced upon binding of ligands by direct competition (Type III) or indirectly through conformational changes caused by binding of certain Type I or Type II ligands to the ATP site. C) The approach involves primary screening to measure ANS displacement potential, a follow-up assay using an ATP site blocker such as staurosporine to classify the hit compounds, a secondary assay to evaluate inhibitory activity, and the determination of the molecular mode of action by protein crystallography.

**A)**

BLANK	1	2	3	4	5	6	7	8	9	10	11	12
A	381	437	517	556	2283	596	619	610	478	646	490	434
B	470	568	633	618	388	539	535	1489	540	492	1604	489
C	596	766	1828	772	1059	1111	645	552	522	2598	471	501
D	496	571	513	659	795	521	783	609	490	643	468	340
E	478	466	575	767	493	530	571	510	636	613	559	423
F	574	544	686	1080	1929	554	632	1341	685	477	490	560
G	437	548	950	659	676	13699	438	508	777	436	596	570
H	591	1122	584	729	696	575	624	679	488	601	454	401

**B)**

RAW	1	2	3	4	5	6	7	8	9	10	11	12
A	924	8037	2670	10231	5466	8693	8904	9293	8272	8987	7798	8198
B	1007	8459	9572	8465	3863	8537	1334	6758	7536	7405	9085	7239
C	901	9158	8558	8879	9119	6452	8962	9246	9147	10240	11696	7898
D	1191	2973	8385	8626	7824	7544	8385	7918	6887	8942	9022	7457
E	7864	8151	7765	8386	12109	8862	9063	8622	9339	9043	8080	1158
F	8236	7594	8400	8897	10182	8124	8159	9425	8789	8154	8451	833
G	7338	8168	6789	7871	8441	18238	8817	8841	8407	8875	8405	1094
H	8289	9213	6049	7942	7927	8133	8190	7941	3886	8408	8665	882

**C)**

DELTA	1	2	3	4	5	6	7	8	9	10	11	12
A	543	7600	2153	9675	3183	8097	8285	8683	7794	8341	7308	7764
B	537	7891	8939	7847	3475	7998	799	5269	6996	6913	7481	6750
C	305	8392	6730	8107	8060	5341	8317	8694	8625	7642	11225	7397
D	695	2402	7872	7967	7029	7023	7602	7309	6397	8299	8554	7117
E	7386	7685	7190	7619	11616	8332	8492	8112	8703	8430	7521	735
F	7662	7050	7714	7817	8253	7570	7527	8084	8104	7677	7961	273
G	6901	7620	5839	7212	7765	4539	8379	8333	7630	8439	7809	524
H	7698	8091	5465	7213	7231	7558	7566	7262	3198	7807	8211	481

**D)**

CORR	1	2	3	4	5	6	7	8	9	10	11	12
A	609	8481	2653	10780	3558	9046	9255	9691	8700	9303	8151	8648
B	603	8801	9981	8755	5763	8928	976	7054	7810	7725	8770	7565
C	343	9359	7533	9061	9306	7346	9308	9709	9647	8759	12538	8286
D	781	2678	8765	8879	7823	7845	8489	8161	7165	9400	9526	7919
E	8242	8567	8022	8525	12951	9307	9478	9054	9717	9416	8394	833
F	8574	7851	8799	19881	9196	8440	8396	9024	9028	9018	9372	308
G	7685	8548	6589	8047	8664	5085	9349	9320	8513	9407	8737	593
H	8639	9025	6127	8143	8083	8457	8439	8539	5498	8713	9172	608

**E)**

% CORR	1	2	3	4	5	6	7	8	9	10	11	12
A	101%	0%	74%	0%	62%	0%	0%	0%	0%	0%	1%	0%
B	100%	0%	0%	0%	32%	0%	96%	15%	5%	6%	0%	8%
C	105%	0%	9%	0%	0%	11%	0%	0%	0%	0%	0%	0%
D	99%	73%	0%	0%	5%	5%	0%	0%	14%	0%	0%	4%
E	0%	0%	2%	0%	0%	0%	0%	0%	0%	0%	0%	98%
F	0%	5%	0%	0%	0%	0%	0%	0%	0%	0%	0%	105%
G	7%	0%	21%	2%	0%	41%	0%	0%	0%	0%	0%	101%
H	0%	0%	28%	1%	1%	0%	0%	0%	36%	0%	0%	101%

**Figure 2. Screening of the NCI library using the CDK2-ANS assay**

Example of a 96-well plate CDK2-ANS assay measured at excitation and emission wavelengths of 405 and 460 nm, respectively. Compounds displaying ANS displacement greater than 60% (hits) are shown in black, along with the controls in columns 1 and 12. A) “BLANK” shows the fluorescence signal produced by ANS and compound in the absence of CDK2. Compounds A5, B8, B11, C3, C10, F5, F8, and G6 are self-fluorescent (~2.5 times greater than control shown in grey). These compounds are not to be discarded, but their displacement capability may be difficult to assess using the experimental conditions. B) “RAW” shows the fluorescence signal upon addition of CDK2, identifying A3, B7, D2, and H9 as potential hits. C) “DELTA” is the result of subtracting “BLANK” from “RAW” (Eqn. 1). D) “CORR” is “DELTA” after correction for the inner-filter effect using Eqn. 2, revealing H9 as an unspecific fluorescence quencher (shown in grey). A5 is also highlighted in grey for reason as discussed above. E) “%CORR” is the displacement potential relative to the positive control (SU9516). From this plate, A3 and B7 were identified as hit compounds **6** and **2** respectively, while D2 was discarded following dose-response assays ( $EC_{50} > 50 \mu M$ ).

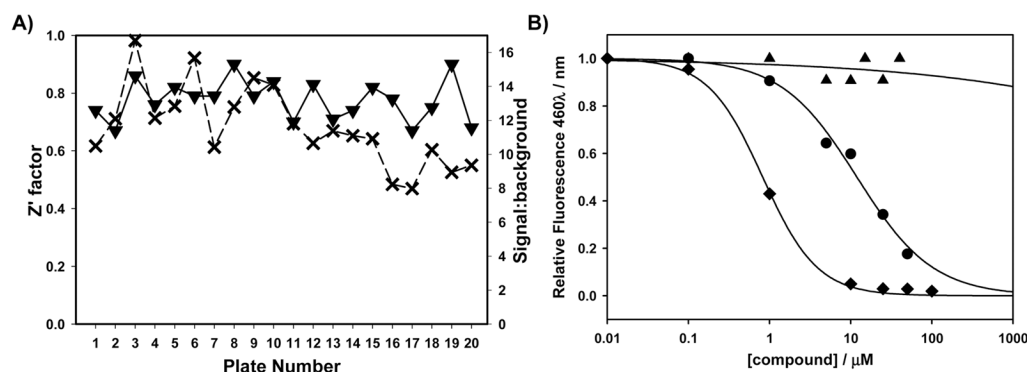


**Figure 3. Assay performance and follow-up assay for classification**

A) Z-factors and signal-to-background ratios corresponding to 96-well low volume format CDK2-ANS assay plates. Average Z-factor value:  $0.8 \pm 0.1$  (▼), average signal-to-background ratio:  $12 \pm 2.3$  (x). B) The use of staurosporine as a non-displacing Type I inhibitor for the classification of Type I/II and Type III in the CDK2-ANS secondary assay. Titration with staurosporine has little effect on the fluorescence yield of the CDK2-ANS complex (▲). Titration of positive control SU9516 in the presence of 10  $\mu\text{M}$  staurosporine showed a 15-fold increase in  $\text{EC}_{50}$  from  $0.8 \pm 0.05 \mu\text{M}$  (◆) to  $12 \pm 1.1 \mu\text{M}$  (●).

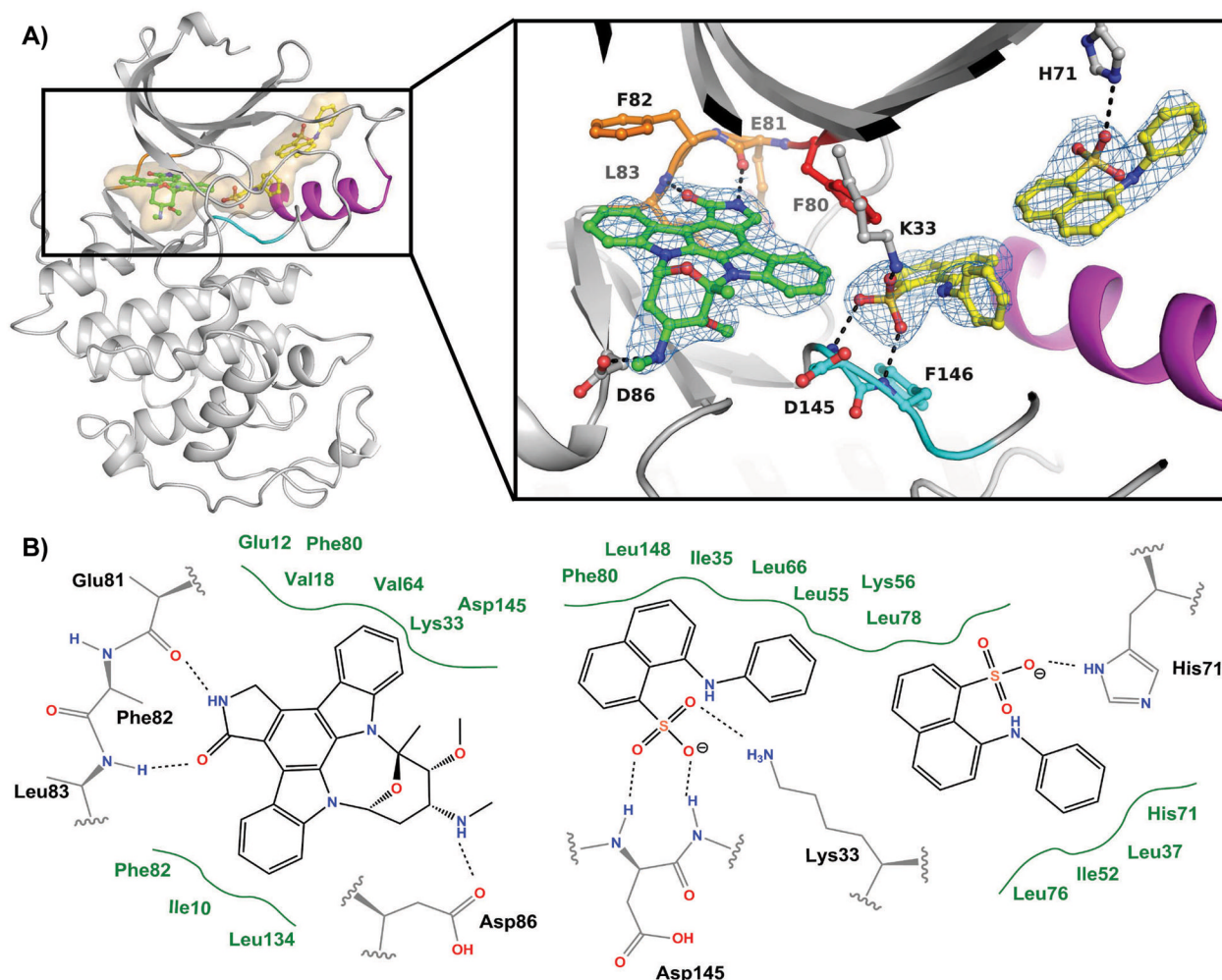


**Figure 4. Ternary structure of CDK2 with staurosporine and ANS**

A) The co-crystal structure of CDK2 liganded with ANS and staurosporine was determined at 2.5 Å resolution (Table 2). Staurosporine (green) binds to the ATP site, along with two ANS molecules (yellow) in the allosteric pocket. The hinge region is shown in orange, the DFG motif in cyan, and the C-helix in magenta. Inset: The 2Fo-Fc electron density map, contoured at 1σ, is shown as blue mesh with hydrogen bonding interactions indicated as black dotted lines. A 1Fo-Fc density map omitting the ligands during refinement is shown in Supplemental Fig. 4. B) Schematic presentation of the binding interactions of staurosporine and ANS in CDK2, with potential van der Waals interactions shown in green.



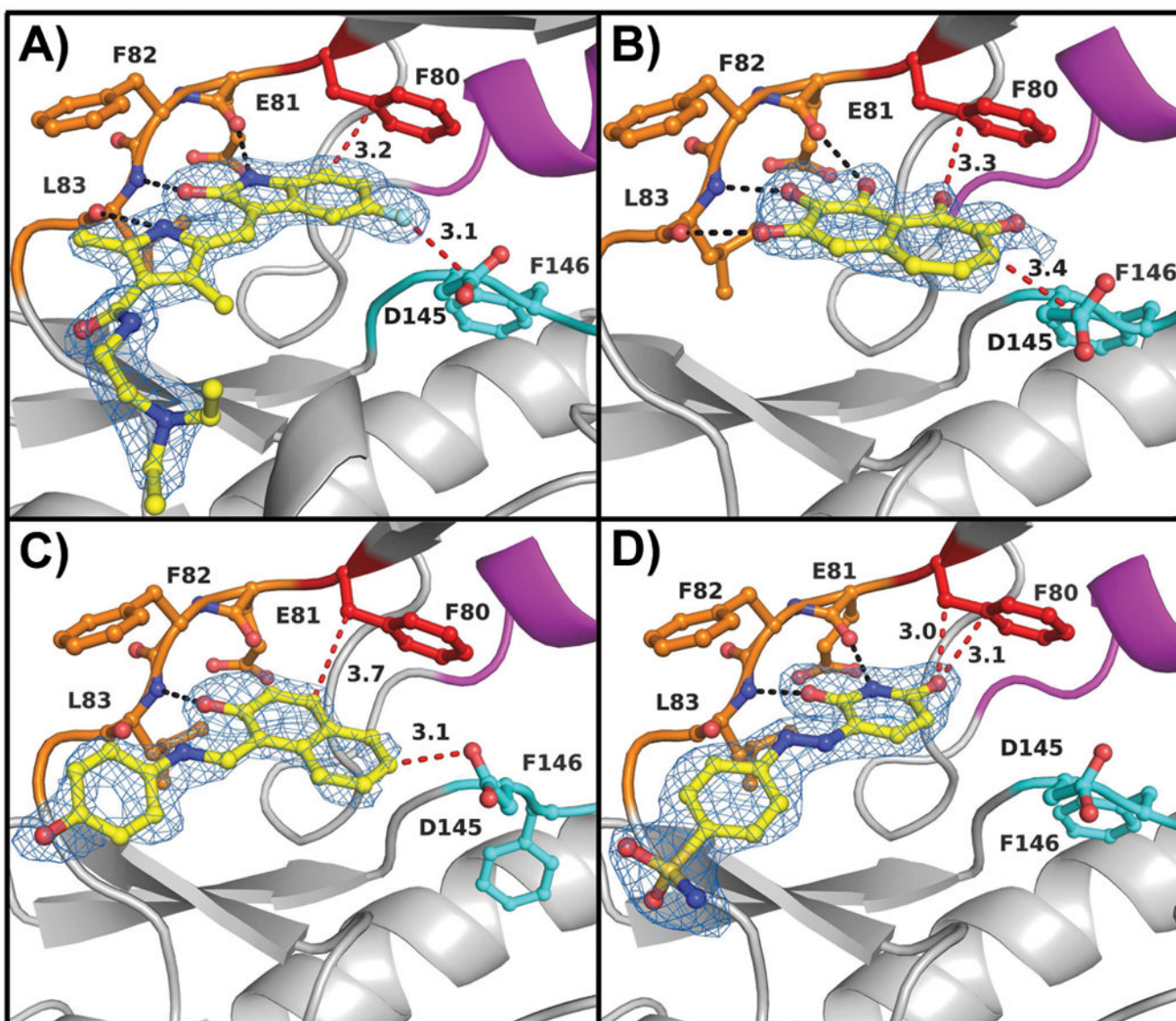


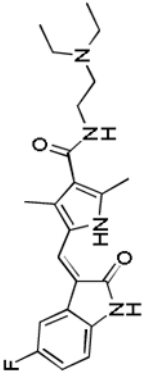
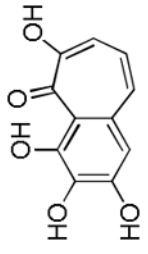
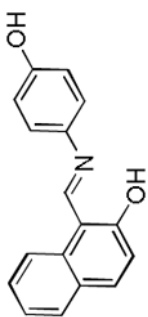
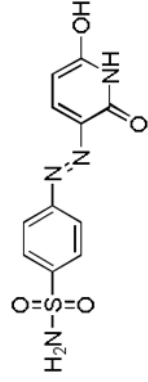
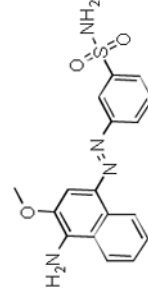
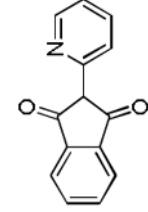
**Figure 5. Molecular mode of action of hit compounds**

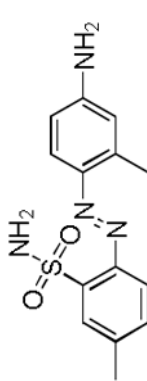
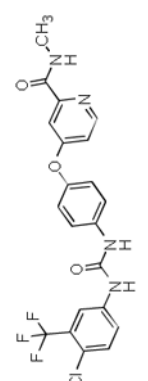
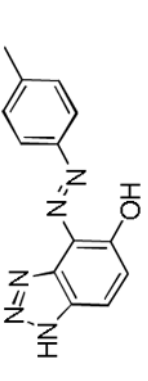
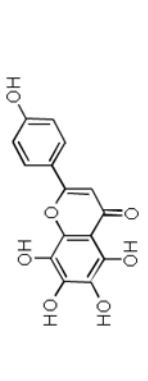
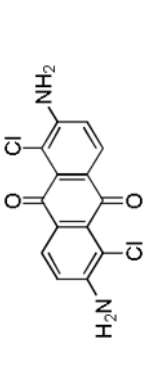
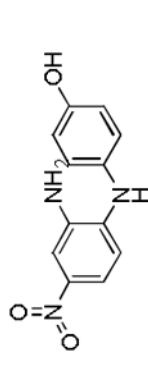
Co-crystal structures with CDK2 were determined for hit compounds A) **1** (sunitinib), B) **2** (purpurogallin), C) **3**, and D) **4** with the hinge region shown in orange, gatekeeper residue Phe80 in red, the DFG motif in cyan, the C-helix in magenta, and the compounds in yellow; the 2Fo-Fc electron density map, contoured at  $1\sigma$ , is shown as blue mesh. The black dotted lines indicate potential hydrogen bonding interactions, and the red dotted lines indicate potential clashes with gatekeeper residue Phe80 and Asp145 of the DFG motif. 1Fo-Fc density maps omitting the ligands during refinement are shown in Supplemental Fig. 5.



Table 1

Hit compounds identified

Hit	Chemical Structure	EC <sub>50</sub> /μM [Staurosporine] <sup>a</sup>			IC <sub>50</sub> /μM <sup>b</sup>
		0 μM	5 μM	10 μM	
1		8.2 ± 0.5	49 ± 8.4	> 100	130 ± 17
2		7.2 ± 0.6	40 ± 2.9	> 100	17 ± 1.3
3		12 ± 0.8	56 ± 8.0	> 100	> 150
4		15 ± 0.7	53 ± 2.9	> 100	45 ± 8.3
5		6.0 ± 0.9	18 ± 2.1	> 100	53 ± 5.7
6		19 ± 0.8	58 ± 9.2	> 100	46 ± 10

Hit	Chemical Structure	EC <sub>50</sub> /μM	Staurosporine <sup>a</sup>	IC <sub>50</sub> /μM <sup>b</sup>
7		15 ± 1.3	67 ± 18	>150
8		14 ± 1.1	38 ± 16	>150
9		16 ± 1.2	66 ± 6.0	>150
10		20 ± 1.8	>100	>150
11		35 ± 6.5	77 ± 23	>150
12		44 ± 5.0	90 ± 9.2	>150

<sup>a</sup> ANS displacement potential in the absence and presence of staurosporine.

<sup>b</sup> Inhibitory potential towards the activated CDK2-cyclin A complex.

Table 2

Summary of data collection and structure refinement.

Hit compound (PDB ID)	1 (3TI1)	2 (3TIY)	3 (3TIZ)	4 (4EZ3)	Staurosporine-ANS (4EZ7)	Staurosporine (4ERW)
Co-crystallization	Sumitinib	NSC 35676	NSC 111848	-	-	-
Soaking	-	-	-	NSC 134199	Staurosporine ANS	Staurosporine
Space group	P2 <sub>1</sub> 2 <sub>1</sub> 2 <sub>1</sub>	P2 <sub>1</sub> 2 <sub>1</sub> 2 <sub>1</sub>	P2 <sub>1</sub> 2 <sub>1</sub> 2 <sub>1</sub>	P2 <sub>1</sub> 2 <sub>1</sub> 2 <sub>1</sub>	P2 <sub>1</sub> 2 <sub>1</sub> 2 <sub>1</sub>	P2 <sub>1</sub> 2 <sub>1</sub> 2 <sub>1</sub>
Unit cell dimensions: a, b, c (Å)	a=53.6	a=53.5	a=53.2	a=53.4	a=53.2	a=53.6
	b=71.9	b=72.0	b=71.9	b=70.4	b=70.2	b=71.3
	c=72.5	c=72.3	c=72.2	c=71.5	c=71.8	c=72.4
Resolution range	20-1.99 (2.05-1.99)	20-1.84 (1.9-1.84)	20-2.02 (2.10-2.02)	20-2.00 (2.10-2.00)	20-2.50 (2.54-2.50)	20-2.00 (2.10-2.00)
Unique reflections	19765 (1666)	24419 (2096)	18724(2022)	18753(2510)	9577(431)	19319(2572)
Completeness (%)	99.8 (99.9)	98.2 (93.2)	99.8 (100)	99.7 (99.9)	97.2 (90.0)	99.8 (100)
I/σI	25 (5.7)	35 (7.6)	21 (4.9)	21 (6.4)	47 (6.7)	29 (6.2)
R <sub>merge</sub> <sup>a</sup> (%)	7.7(35.7)	4.4 (23.5)	8.4 (33.3)	6.4 (35.9)	6.6 (30.4) #	6.8 (28.0)
Protein atoms	2370	2369	2358	2367	2439	2361
Average B-factor (Å <sup>2</sup> )	34	29	31	35	39	34
Inhibitor molecules	29	16	20	20	77	35
Average B-factor (Å <sup>2</sup> )	34	39	34	28	41	29
Ligand(s) atoms	32	48	32	4	16	64
Average B-factor (Å <sup>2</sup> )	33	40	34	21	37	39
Solvent molecules	97	151	97	97	40	115
Average B-factor (Å <sup>2</sup> )	30	30	28	31	28	33
Rmsd <sup>b</sup> bonds (Å)	0.008	0.009	0.007	0.014	0.007	0.015
Rmsd angles (°)	1.2	1.3	1.2	1.7	1.1	1.5

Hit compound (PDB ID)	1 (3TII)	2 (3TIY)	3 (3TIZ)	4 (4EZ3)	Staurosporine-ANS (4EZ7)	Staurosporine (4ERW)
$R_{\text{crist}}$ (%) <sup>c</sup>	20.5	18.4	19.3	21.5	22.0	19.6
$R_{\text{free}}$ (%) <sup>d</sup>	26.2	22.4	24.3	25.1	27.4	24.4
$R_{\text{free}}$ reflection set size	990 (5.0 %)	1100 (4.5 %)	938 (5.0 %)	937 (5.0 %)	370 (4.0 %)	966 (5.0 %)
Coordinate error (Å) (ML method from PHENIX)	0.18	0.20	0.23	0.20	0.29	0.22

<sup>a</sup> $R_{\text{merge}}$  = quality of amplitudes ( $F$ ) in the scaled data set, Diederichs & Karplus (1997), Nature Struct. Biol. 4, 269–275.  
<sup>b</sup>r.m.s.d. = root mean square deviation from ideal values.  
<sup>c</sup> $R_{\text{crist}} = 100 \times \sum |F_{\text{obs}} - F_{\text{model}}| / F_{\text{obs}}$  where  $F_{\text{obs}}$  and  $F_{\text{model}}$  are observed and calculated structure factor amplitudes, respectively.  
<sup>d</sup> $R_{\text{free}}$  is  $R_{\text{crist}}$  calculated for randomly chosen unique reflections, which were excluded from the refinement.  
<sup>#</sup> $R_{\text{sym}} (\text{HKL200}) = \text{SUM} (\text{ABS}(1 - \langle I \rangle)) / \text{SUM} (I)$